

Effects of nasal septum perforation repair surgery on three-dimensional airflow: an evaluation using computational fluid dynamics

Tsutomu Nomura · Munetaka Ushio ·
Kenji Kondo · Tatsuya Yamasoba

Received: 8 October 2014 / Accepted: 7 December 2014 / Published online: 13 December 2014
© Springer-Verlag Berlin Heidelberg 2014

Abstract The purpose of this research is to determine the cause of nasal perforation symptoms and to predict post-operative function after nasal perforation repair surgery. A realistic three-dimensional (3D) model of the nose with a septal perforation was reconstructed using a computed tomography (CT) scan from a patient with nasal septal defect. The numerical simulation was carried out using ANSYS CFX V13.0. Pre- and post-operative models were compared by their velocity, pressure gradient (PG), wall shear (WS), shear strain rate (SSR) and turbulence kinetic energy in three plains. In the post-operative state, the crossflows had disappeared, and stream lines bound to the olfactory cleft area had appeared. After surgery, almost all of high-shear stress areas were disappeared comparing pre-operative model. In conclusion, the effects of surgery to correct nasal septal perforation were evaluated using a three-dimensional airflow evaluation. Following the surgery, crossflows disappeared, and WS, PG and SSR rate were decreased. A high WS, PG and SSR were suspected as causes of nasal perforation symptoms.

Keywords Nasal septal perforation · Airflow evaluation · Numerical simulation

Introduction

Nasal septal perforation can be caused by septal surgery, hemostat to nasal bleeding, tumor removal in the septal

area, excessive nose picking, and cocaine use. Patients may have a variety of symptoms, such as nasal bleeding, crust formation, nasal stuffiness and whistling noise. These symptoms are irritating for the patients and they are sustained until the defect is corrected [1, 2]. The mechanisms causing the symptoms of nasal septal perforation have not been fully elucidated. Some reports have shown that septal perforation causes abnormal airflow using a computer simulation of the airway [3–6] but it should be noted that all these simulations were performed using an artificial perforation. In the current study, we analyzed the effects of nasal septum perforation repair on three-dimensional airflow using perforation model reconstructed based on computed tomography (CT) data of a patient, and tried to determine the causes of nasal perforation symptoms and to predict the post-operative nasal function.

Materials and methods

Patient

A 51-year-old female patient visited our hospital complaining of repetitive nasal bleeding, nose stuffiness and crusta formation. During the nasal examination, a perforation 20 mm in diameter was found in the anterior nasal septum (Fig. 1a, b). All of her symptoms were thought to be related to the septal perforation, and repair surgery was planned and performed. The procedure started with the elevation of bilateral mucosal flaps under an endoscopic view. A releasing incision was made across the nasal floor on one side and across the lateral cartilage on the other side. The flaps were slid up- and down-ward, respectively. The perforation is then sutured. After surgery, all symptoms were apparently resolved, given that the patient had

T. Nomura (✉) · M. Ushio · K. Kondo · T. Yamasoba
Department of Otolaryngology and Head and Neck Surgery,
Graduate School of Medicine, The University of Tokyo,
7-3-1 Hongo, Bunkyo-ku, Tokyo, Japan
e-mail: t-nomura@bc5.so-net.ne.jp



Fig. 1 **a** Pre-operative state of nasal septal perforation. Diameter of perforation is almost 20 mm. *S* septum, *IT* inferior turbinate. **b** Reconstruction cut-model of pre-operative state. **c** Reconstruction cut-model of post-operative state

no more symptoms when she was evaluated 12 months after surgery. The effect of nasal perforation repair on three-dimensional airflow was evaluated on the model based on CT data from this patient.

Model generation

A realistic three-dimensional (3D) model of the nose with a septal perforation was reconstructed using CT scans of the patient with 0.5 mm thick slices. The data were transferred by DICOM data, and the nasal geometry was determined using INTAGE Volume Editor (CYBERNET SYSTEMS CO., LTD. Tokyo, Japan). The geometry was meshed using ICEM-CFD (ANSYS, Inc. Canonsburg, PA, USA), and the numerical simulation was performed using ANSYS CFX V13.0 (ANSYS, Inc. Canonsburg, PA, USA).

The post-operative model was constructed from the pre-operative CT scan using ICEM-CFD, referring to the post-operative nose condition. For the ICEM-CFD simulation, the flow was assumed to be incompressible, in a quasi-state and at a temperature of 25 °C. To account for the possible existence of turbulence, κ - ϵ (kappa-epsilon) model was used. This model comprised about one million tetrahedral grids.

As of boundary conditions, the nasal walls were assumed to be a non-slip, rigid model. A velocity of 2 m/s airflow was applied to the outlet surface, and zero gauge pressure was applied to the pressure inlet as atmospheric pressure (Fig. 2).

Analysis

Pre and post-operative models were compared for the stream line velocity, pressure gradient (PG), wall shear (WS), shear stress transport (SSR) and turbulence kinetic energy in three planes (Fig. 3).

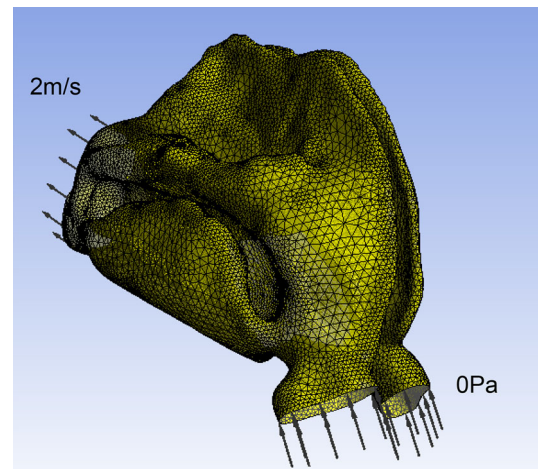


Fig. 2 Boundary conditions on 3D mesh model 0 Pa at the inlet and 2 m/s airflow at the outlet

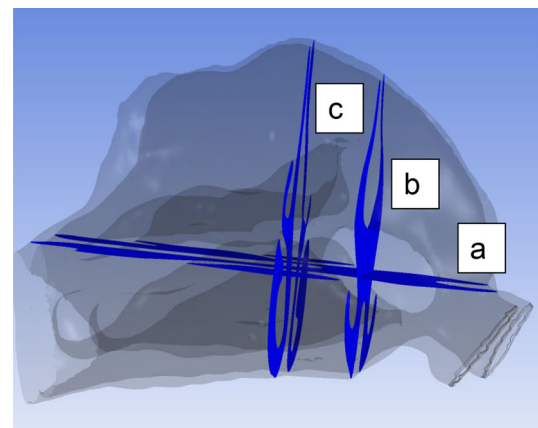


Fig. 3 The three planes that were evaluated **a** parallel plane to Frankfurt plane crossing center of septal perforation. **b** Perpendicular plane to Frankfurt plane crossing center of septal perforation. **c** perpendicular plane to Frankfurt plane crossing the olfactory area

Results

The velocity of pre- and post-operative state in the stream line view is shown in Fig. 4. In the pre-operative state, air flow passes thorough across the septal perforation to another side. The maximum speed was recorded 8.9 m/s at the nostrils and the left inferior meatus area. In the post-operative state, the crossflow disappeared. The maximum post-operative speed was 9.18 m/s, which was recorded at same area as in the pre-operative state.

Stream lines bound to the olfactory cleft area appeared post-operatively (Fig. 4, Arrow).

The WS is shown in Fig. 5, and high score points in lateral wall behind perforation and right nostril area seen in plane parallel to Frankfurt plane was disappeared after surgery.

But, high score points appeared in right upper septal wall and surface of right inferior turbinate.

The PG distribution is shown in Fig. 6. In pre-operative state, the posterior, superior and inferior edges of the

perforation had high PG. After surgery, the area of the high PG was cleared in posterior, superior and inferior areas, while high gradient newly appeared in surface of right inferior turbinate in post-operative model.

The SSR is shown in Fig. 7. In pre-operative state, the posterior wall and nostril areas had high SSR. After surgery, SSR was reduced in posterior area, but left side repaired septal wall had slightly higher SSR than right side septal wall. In addition, there was no significant difference in turbulence kinetic energy before and after surgery (Fig. 8).

In olfactory are, heterogeneity of velocity was found in pre-operative state, but velocity was almost same in pre and post-operative state (Fig. 9).

Discussion

Septal perforation causes irritating symptoms for patients. However, there are few scientific explanations for the

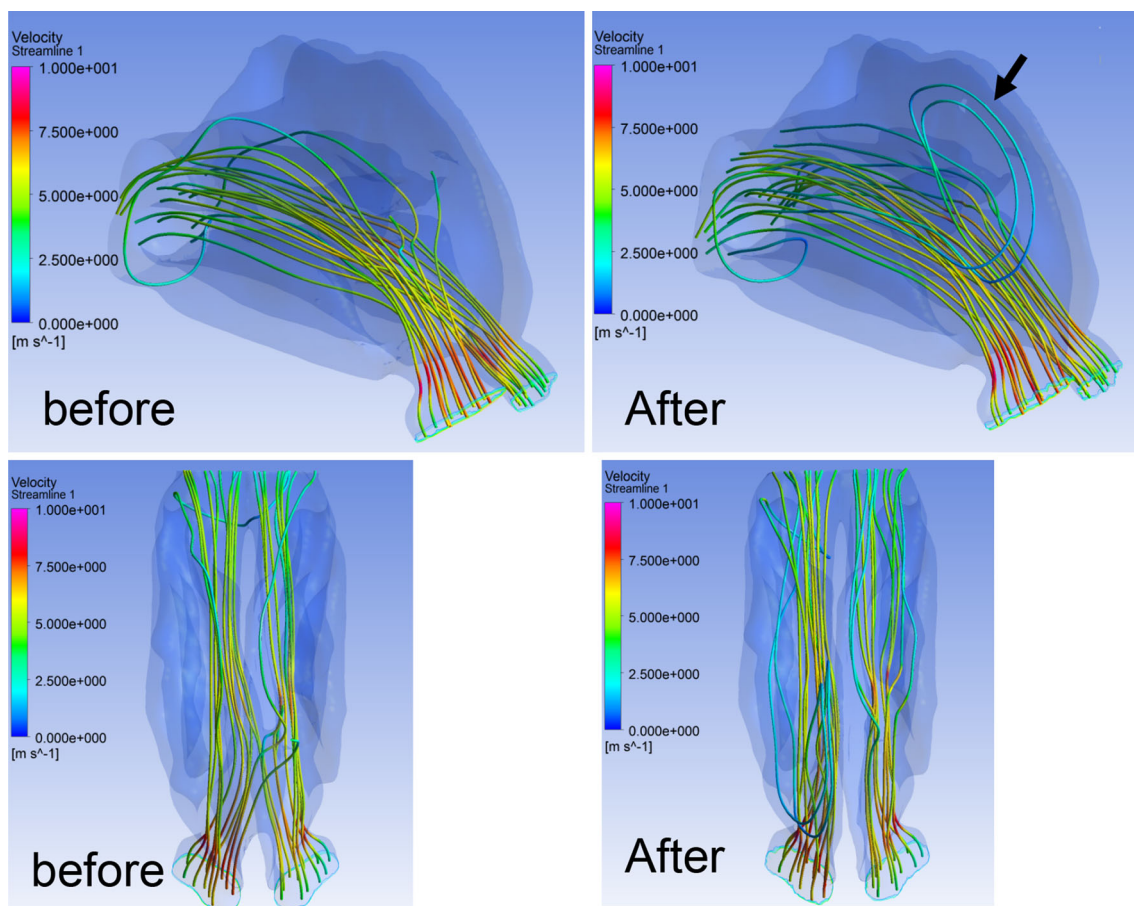


Fig. 4 Velocity stream line. In the pre-operative state (*right side*), air flow passes thorough across the septal perforation to another side. In the post-operative state (*left side*), the crossflow disappeared. And

stream lines bound to the olfactory cleft area appeared (*Arrow*). The nasal cavities are viewed from the superior aspect (*bottom*)

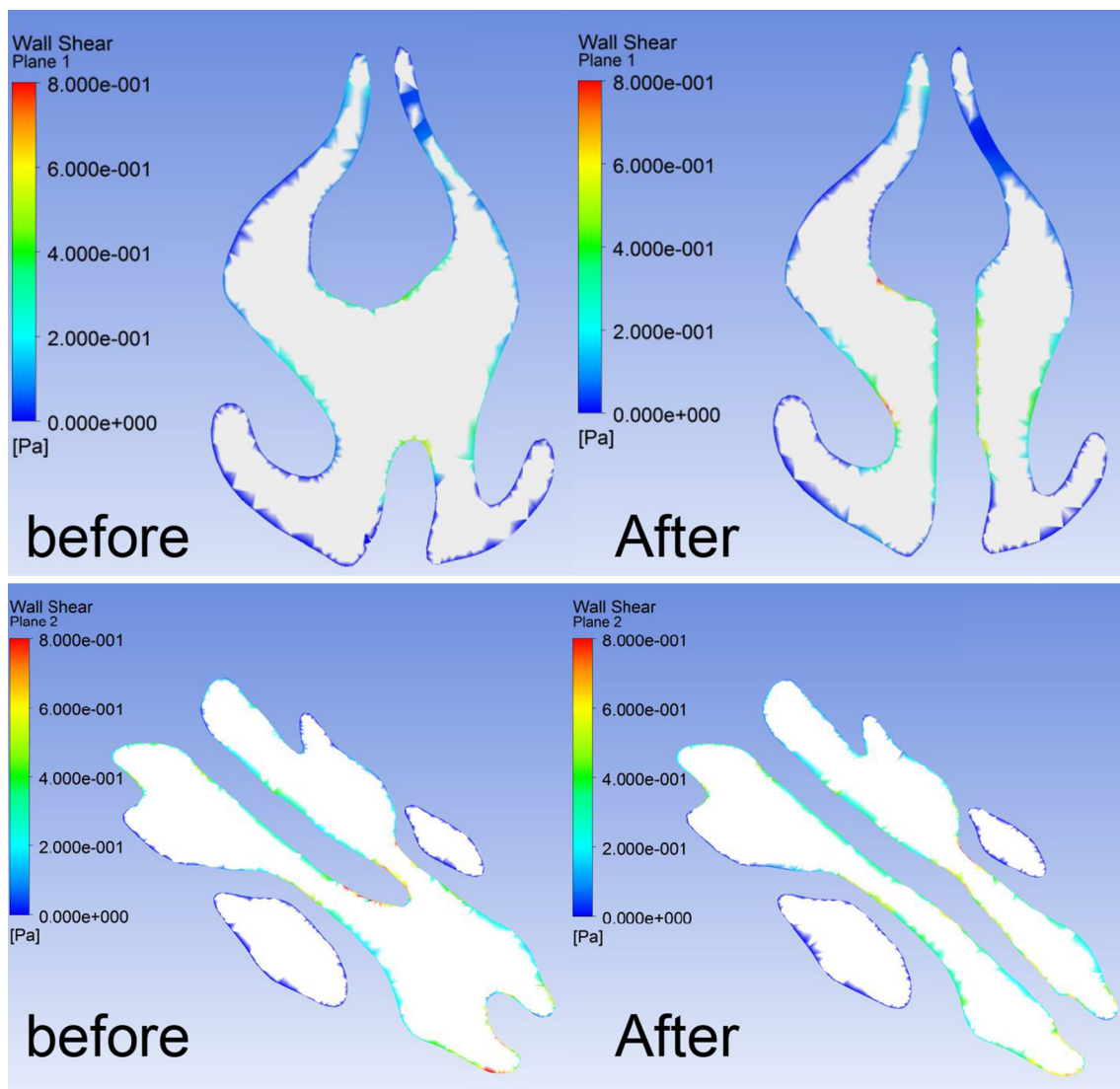


Fig. 5 Wall shear. High score points in lateral wall behind perforation and right nostril area seen in plane parallel to Frankfurt plane (*left bottom*) was disappeared after surgery (*right bottom*). New high score

points appeared in right upper septal wall and surface of right inferior turbinate (*right top*)

causes of these symptoms. To evaluate the mechanisms for the causes of these symptoms, a nasal air flow analysis has been performed. A nasal obstruction model described by Rhee et al. [7] and Chen et al. [8] was designed to evaluate the effect of septal repair surgery, and this model showed the effectiveness of using computer fluid dynamics (CFD).

For model reconstruction, we used an κ - ϵ model, which took turbulent airflow into consideration. In our model, we applied airflow with a velocity of 2 m/s at the outlet, which was similar to the 50 Pa applied by Grant et al. [3] and Lee et al. [5]. In addition, the maximum velocity used in Grant's model was 12 m/s [5], which is similar to the

maximum velocity used in our study. However, in our study, turbulence was not observed in pre- or post-operative models. In contrast, Wang [9] found the turbulent flow at flow rate of 30 L/min. This flow rate corresponds to a velocity of 8.3 m/s at the outlet in our model. The rate used by Wang [9] is considered too fast to directly compare with our rate of 2 m/s, and this may be the cause of appearance of turbulence. Turbulent airflow should, however, be considered for a more precise simulation.

In the stream line view, the crossflow disappeared after surgery, and similar to other studies [3–5] a high flow rate was recorded in post-operative model. These findings

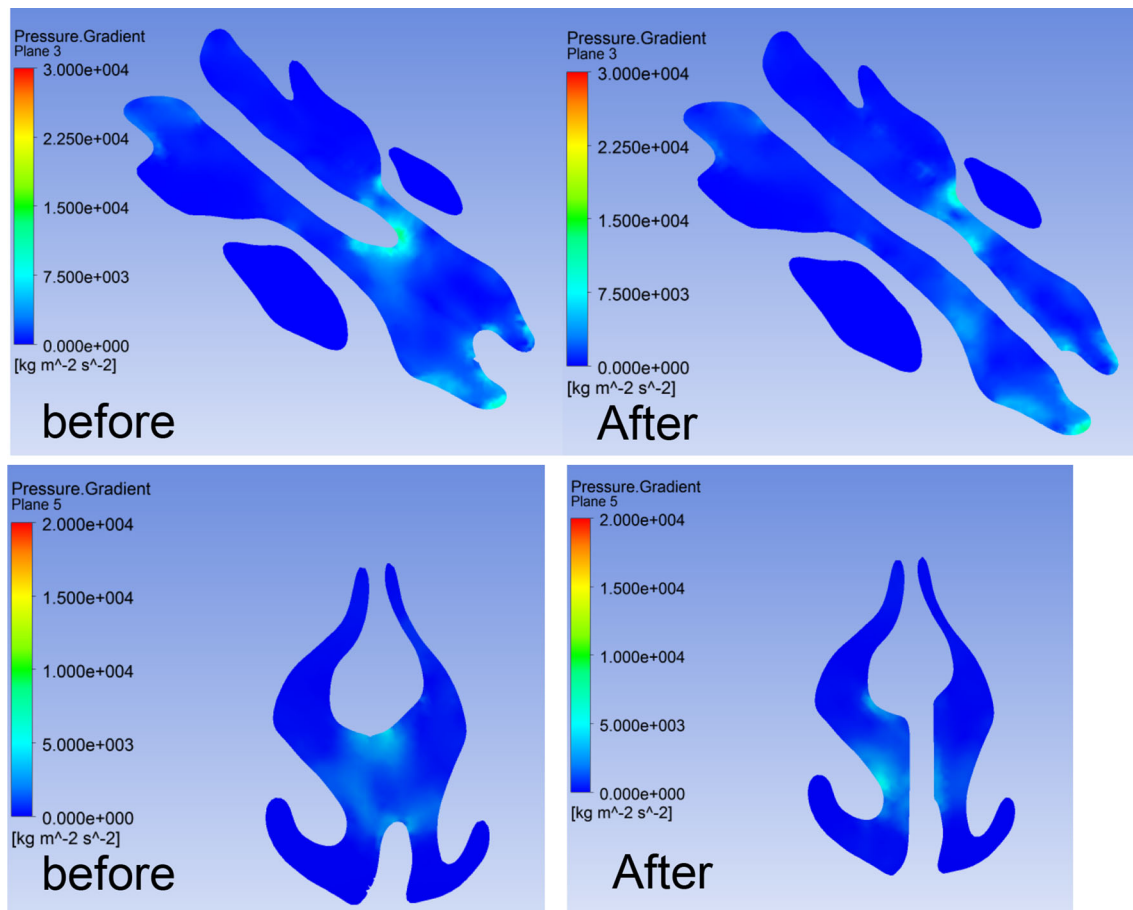


Fig. 6 Pressure gradient In pre-operative state, the posterior, superior and inferior edges of the perforation had high PG (*left top and bottom*). After surgery, the area of the high PG was cleared in

posterior, superior and inferior areas, while high gradient newly appeared in surface of right inferior turbinate in post-operative model (*right top and bottom*)

suggest that septal perforation prevents to provide physiological velocity, which may be a cause of nasal stuffiness sensation. Furthermore, in the upper nasal area, some air flow appeared in post-operative model. This suggests that there is a chance of the patient to improve olfactory function after surgery.

The WS was used by several researchers [3, 5] to evaluate the extent of nasal membrane damage. In this study, high score points in lateral wall was decreased by surgery. PG and SSR were concentrated in the posterior area in both models. These findings suggest that not only WS, PG and SSR are decreased by surgery. Because PG and SSR are presenting a deviation of pressure or stress, these expressions are different from pressure or stress. There are some studies for hemodynamic damage to the artery. WS gradient or PG are suggested as mechanical

trigger of damage of arterial wall [10, 11]. Thus, this heterogeneity of PG and SSR in our study are thought to cause mucosal damage as well as WS.

Some studies [4, 5] showed a very high WS in the edge area of the perforation, while we found lateral wall behind perforation. This difference may be due to the difference in model used. The high WS in the edge areas could result from the sharp edges on the artificial perforations. However, we used a model based on data from a patient with a septal perforation, which resulted in smooth edges in our model; sharp edges compared to smooth edges might account for the differences observed between other studies [3, 4] and ours.

In the current study, we presented the usefulness of CFD for nasal septal perforation repair using a perforation model based on an actual septal defect in a patient. A further

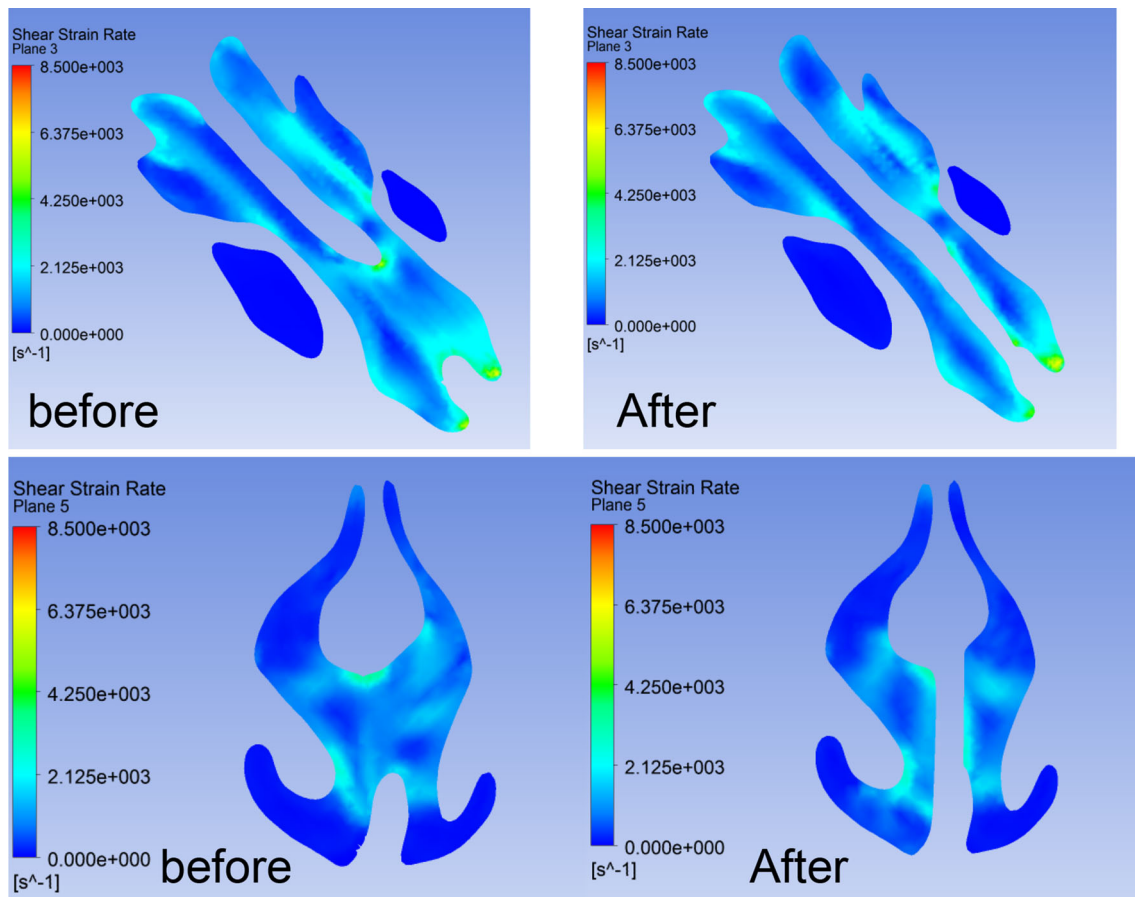


Fig. 7 Shear strain rate In pre-operative state, the posterior wall and nostril areas had high SSR (*left top*). After surgery, SSR was reduced in posterior area, but left side repaired septal wall had slightly higher SSR than right side septal wall (*right top and bottom*)

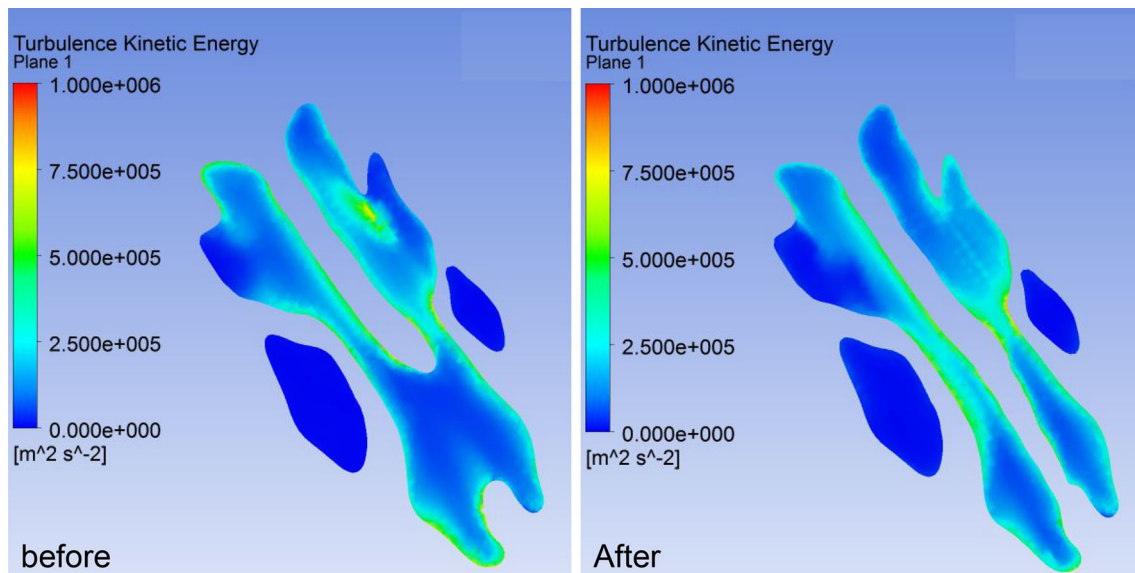


Fig. 8 Turbulence Kinetic Energy. There was no significant difference in turbulence kinetic energy before and after surgery

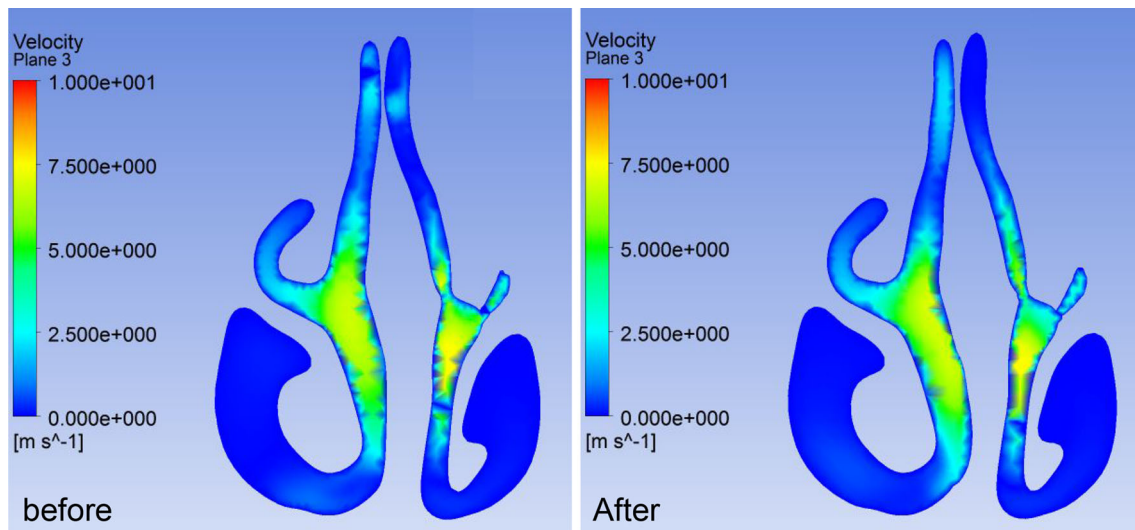


Fig. 9 Velocity in olfactory area. In olfactory are, heterogeneity of velocity was found in pre-operative state (*left side*), but velocity was almost homogeneous (*right side*)

research comparing airflow and stress distribution using a real post-operative model is required to confirm our results, and also we need to collect more cases.

Conflict of interest None.

Ethical standard Patient understood the aim of our study and signed the informed consent.

References

1. Yenigun A, Meric A, Verim A, Ozucer B, Yasar H, Ozkul MH (2012) Septal perforation repair: mucosal regeneration technique. *Eur Arch Otorhinolaryngol* 269:2505–2510
2. Kim SW, Rhee CS (2012) Nasal septal perforation repair: predictive factors and systematic review of the literature. *Curr Opin Otolaryngol Head Neck Surg* 20:58–65
3. Grant O, Bailie N, Watterson J, Cole J, Gallagher G, Hanna B (2004) Numerical model of a nasal septal perforation. *Stud Health Technol Inform* 107:1352–1356
4. Pless D, Keck T, Wiesmiller KM, Lamche R, Aschoff AJ, Lindemann J (2004) Numerical simulation of airflow patterns and air temperature distribution during inspiration in a nose model with septal perforation. *Am J Rhinol* 18:357–362
5. Lee HP, Garlapati RR, Chong VF, Wang DY (2010) Effects of septal perforation on nasal airflow: computer simulation study. *J Laryngol Otol* 124:48–54
6. Cannon DE, Frank DO, Kimbell JS, Poetker DM, Rhee JS (2013) Modeling nasal physiology changes due to septal perforations. *Otolaryngol Head Neck Surg* 148:513–518
7. Rhee JS, Pawar SS, Garcia GJ, Kimbell JS (2011) Toward personalized nasal surgery using computational fluid dynamics. *Arch Facial Plast Surg* 13:305–310
8. Chen XB, Lee HP, Chong VF, de Wang Y (2009) Assessment of septal deviation effects on nasal air flow: a computational fluid dynamics model. *Laryngoscope* 119:1730–1736
9. de Wang Y, Lee HP, Gordon BR (2012) Impacts of fluid dynamics simulation in study of nasal airflow physiology and pathophysiology in realistic human three-dimensional nose models. *Clin Exp Otorhinolaryngol* 5:181–187
10. Li ZY, Taviani V, Tang T, Sadat U, Young V, Patterson A, Graves M (2009) The mechanical triggers of plaque rupture: shear stress vs pressure gradient. *Br J Radiol* 82(Spec 1):S39–S45
11. Finol EA, Amon CH (2002) Flow-induced wall shear stress in abdominal aortic aneurysms: part I—steady flow hemodynamics. *Comput Methods Biomech Biomed Engg* 5:309–318